ISTITUTO NAZIONALE DI FISICA NUCLEARE

Laboratori Nazionali di Frascati

(DRAFT) MEMO for SuperB Steering Committee

INFN/code-08/?
4 Aprile 2008
SuperB-A1-Note

PRELIMINARY RESULTS FROM DAΦNE UPGRADE AS A PROOF OF PRINCIPLE OF NEW CONCEPTS FOR *SuperB*

D. Alesini, M. Biagini, C. Biscari, R .Boni, M. Boscolo, F. Bossi, B. Buonomo, A. Clozza, G. Delle Monache, T. Demma, E. Di Pasquale, G. Di Pirro, A. Drago, A. Gallo, A. Ghigo, S. Guiducci, C. Ligi, F. Marcellini, G. Mazzitelli, C. Milardi, F. Murtas, L. Pellegrino, M. Preger, L. Quintieri, P. Raimondi, R. Ricci, U. Rotundo, C. Sanelli, M. Serio, F. Sgamma, B. Spataro, A. Stecchi, A. Stella, S. Tomassini, C. Vaccarezza, M. Zobov
INFN-Laboratori Nazionali di Frascati Via E. Fermi 40, I-00044 Frascati, Italy
Simona Bettoni
CERN CH-1211, Geneva 23, Switzerland
I.Koop, E. Levichev, P. Piminov, D. Shatilov , V. Smaluk
Budker Institute of Nuclear Physics, Novosibirsk, R- 630090, *Russia*
K. Ohmi
KEK, Ibaraki 305-0801, Japan
N. Arnaud, D. Breton, P. Roudeau, A. Stocchi, A. Variola, B. F. Viaud
Laboratoire de l'Accelerateur Lineaire, 91898 Orsay cedex, France
Marco Schioppa
INFN-Gruppo di Cosenza, Arcavacata di Rende (Cosenza), I-87036, Italy
M.A.Giorgi, E. Paoloni
INFN-Sezione di Pisa, Dip. Fisica Università di Pisa, I-56127 Pisa, Italy
P. Valente
INFN-Sezione di Roma, I-00185 Roma, Italy
M. Esposito
Dip. Fisica Università di Roma La Sapienza, I-00185 Roma, Italy
P. Branchini
Dip. Fisica Università di Roma3, I-00154 Roma, Italy

Abstract

Preliminary results of the upgraded DAΦNE commissioning with *"crab waist"* collision scheme are reported here, with a discussion on the application to the *SuperB.*

PACS.:

Presented to R- ECFA (Lisbon -March29,2008)

Published by ***SIS–Pubblicazioni***
Laboratori Nazionali di Frascati

1 INTRODUCTION

DAΦNE is a symmetric e^+ e^- collider designed to run with high luminosity in the energy range of the Φ resonance (1.02 GeV). The DAΦNE complex consists of a Linac for e^+ and e^-, a Damping Ring for both beams, used to decrease their emittances for injection into the Main Rings, and two horizontally separated Main Rings, colliding in one or two Interaction Points.

The operations for the KLOE experiment ended in 2005, culminating with a maximum peak luminosity of 1.5 $10^{32}cm^{-2}s^{-1}$. During the subsequent operations with similar beam conditions for the FINUDA experiment (hypernuclei production) a peak luminosity of 1.6 $10^{32}cm^{-2}s^{-1}$ was achieved with a finer tuning of the optics. In Fig. 1 are the best operation days for both experiments, when integrated luminosity was hitting the record value of about 10 pb^{-1}.

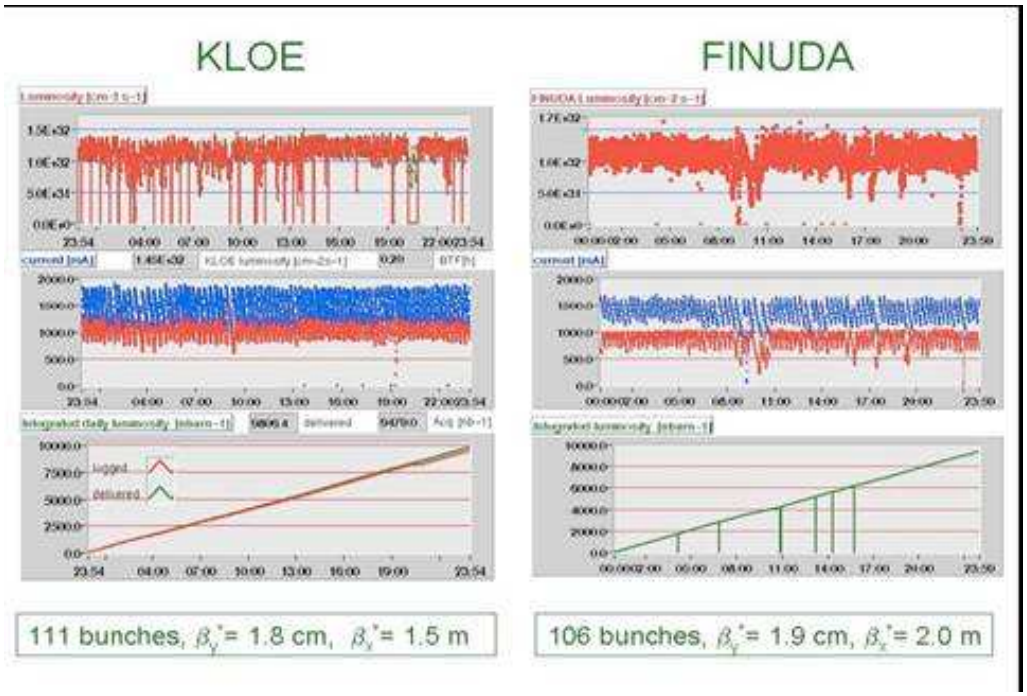

FIG. 1: KLOE and FINUDA best days.

The DAΦNE upgrade aims at increasing the peak luminosity by a factor between 2 and 6, exploiting the novel concepts developed for SuperB, i.e. low emittance beams, large Piwinsky angle and *crab waist*. Hence the achievement of the DAΦNE luminosity goal is a crucial milestone in the *SuperB* program.

2 THE LARGE CROSSING ANGLE AND CRAB WAIST CONCEPTS

High luminosity can be achieved in colliders acting on the parameters as in the following formula:

$$L = f_{coll} \quad \frac{N^+ N^-}{4\pi \sigma_x \sigma_y} \quad R_l \tag{1}$$

where f_{coll} is the collision frequency, N^+ and N^- are the number of particles per beam, σ_x and σ_y are respectively horizontal and vertical rms beam sizes and R_l is a reduction factor which takes into account geometrical and "hourglass" effects.

The approach chosen by KEKB Super B-Factory for luminosity upgrade is to shorten the bunches to 3 mm, decrease the beam emittances and betatron functions at the IP, so decreasing beam sizes, and increase the beam currents ("ultra-high current scheme", 9.4 A and 4.1 A for LER and HER) [1]. The short bunch length allows to decrease β_y* at the IP, without incurring in the "hourglass" effect.

The option chosen for SuperB to produce a peak luminosity in excess of 10^{36} $cm^{-2}s^{-1}$ is based on the "*crab waist*" (*CW*) scheme [2] for beam-beam collisions which combines several potentially advantageous ideas. This option is now being applied to the upgraded DAΦNE Φ-Factory at LNF, Frascati.

The first ingredient of this scheme is the large Piwinski angle: for collisions under a crossing angle θ the luminosity L and the horizontal ξ_x and the vertical ξ_y tune shifts scale as (see for example in [3]):

$$L \propto \frac{N\xi_y}{\beta_y} \tag{2}$$

$$\xi_y \propto \frac{N\sqrt{\beta}_y}{\sigma_x\sqrt{1+\phi^2}} \approx \frac{2N\sqrt{\beta}_y}{\sigma_z\theta} \tag{3}$$

$$\xi_x \propto \frac{N}{\sigma_x^2\left(1+\phi^2\right)} \approx \frac{4N}{\left(\sigma_z\theta\right)^2} \tag{4}$$

Piwinski angle ϕ is defined as:

$$\phi = \frac{\sigma_z}{\sigma_x} tg\left(\frac{\theta}{2}\right) \approx \frac{\sigma_z}{\sigma_x}\frac{\theta}{2} \tag{5}$$

σ_x being the horizontal rms bunch size, σ_z the rms bunch length, N the number of particles per bunch. Here we consider the case of flat beams, small horizontal crossing angle $\theta << 1$ and large Piwinski angle $\phi >> 1$. In the *CW* scheme the large Piwinski angle is obtained by decreasing the horizontal beam size and increasing the crossing angle. As a result, both luminosity and horizontal tune shift increase, and the overlap area of the colliding bunches is decreased proportionally to σ_x/θ. So, if the vertical beta function β_y is comparable to the overlap area size:

$$\beta_y \approx \frac{\sigma_x}{\theta} << \sigma_z \tag{6}$$

several advantages follow:

a) small spot size at the IP, i.e. higher luminosity (see eq. (2)),
b) reduction of the vertical tune shift (see eq. (3))
c) suppression of the vertical synchrobetatron resonances [4].

In addition, in such a collision scheme there is no need of decreasing the bunch length to gain luminosity, then relaxing the problems of HOM heating, coherent synchrotron radiation of short bunches and excessive power consumption.

Long-range beam-beam interactions are expected to limit the maximum achievable luminosity when the bunch distance is short (the so called "parasitic collisions", PC). Thanks to the large crossing angle and small horizontal beam size in the *CW* scheme, the beams separation at the PC is large in terms of σ_x, automatically solving this problem.

The choice of large Piwinski angle, beneficial to the luminosity, introduces new beam-beam resonances and may strongly limit the maximum tune shifts achievable (see for example in [5]). The *CW* transformation is expected to solve such a problem. It actually contributes to suppress, through the vertical motion modulation by the horizontal oscillations, betatron and synchrobetatron resonances usually arising in collisions without *CW*. The *CW* scheme is realized by a couple of sextupole magnets on the two sides of the IP, as shown in Fig. 2. To provide the exact compensation the sextupoles must have a phase advance with respect to the IP of π the horizontal plane and at $\pi/2$ in the vertical one.

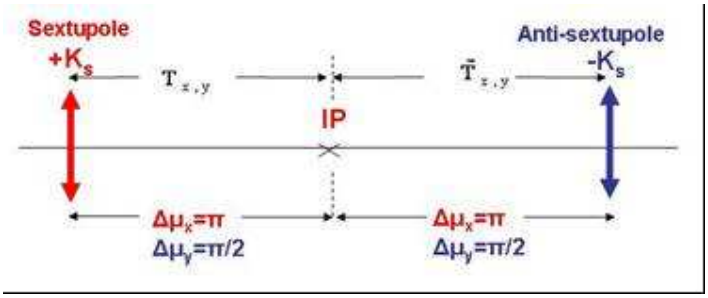

FIG. 2: *Crab waist* correction by sextupole lenses.

As an example of how the *CW* transformation actually works, Fig.3 below shows the *SuperB* bunch charge density envelopes at the IP when colliding without (top) and with (bottom) the *CW* sextupoles. In red is the Low Energy Beam, in blue the High Energy one, whom distribution is shown only near the overlap region. For sake of clarity, in the picture the crossing angle has been reduced by a factor of 4, to enhance the *CW* transformation effect.

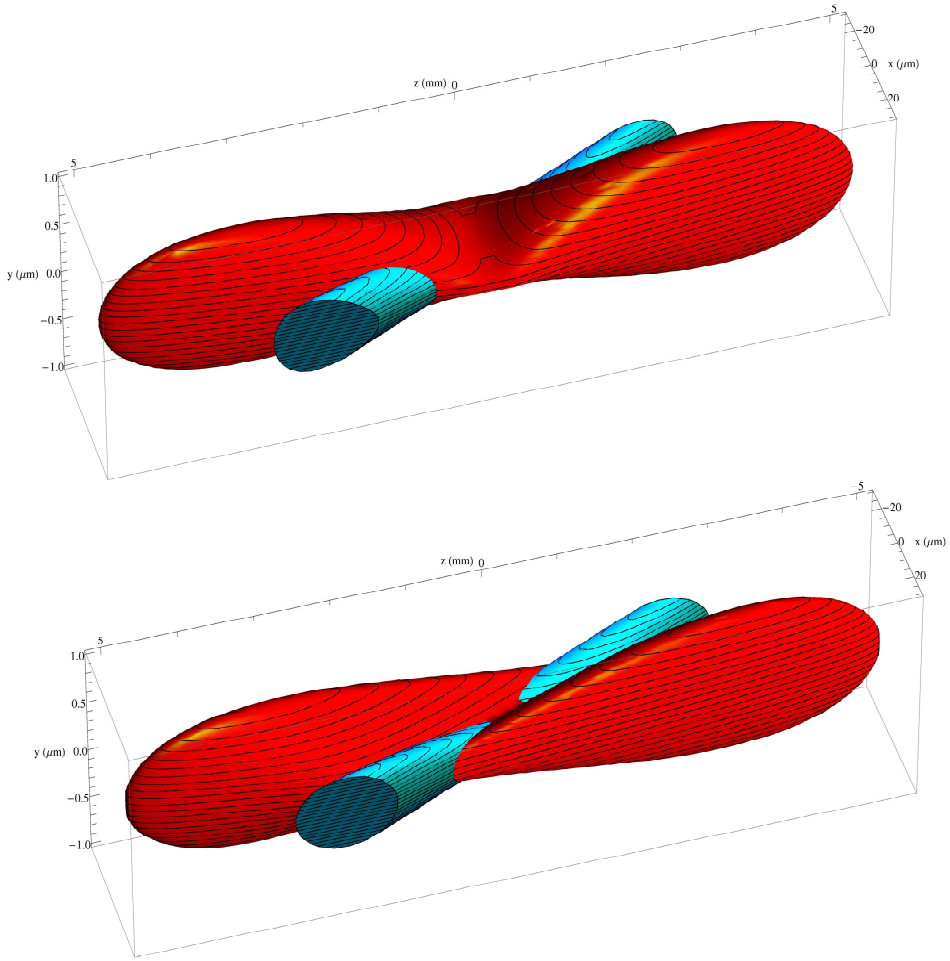

FIG. 3: Sketch of the large Piwinski angle and *crab waist* scheme for *SuperB*. Top: *CW* transformation OFF. Bottom: *CW* transformation ON.

The contour lines are points with the same y coordinate. When there is no *CW* transformation (top plot) the waist line is orthogonal to the axis of one bunch (LEB in this example). Otherwise, when the *CW* transformation is on (bottom plot) the waist moves to the axis of the other beam (HEB here). As a consequence, each beam collides with the other in the minimum β_y region, with a net luminosity gain. Actually, besides the geometrical gain just mentioned, because of the *CW* transformation the non linear component of the beam-beam forces decreases, hence reducing the emittance growth due to the collision. The *CW* transformation acts on the y-plane as described by the following formula:

$$y \quad \rightarrow \quad y - \chi x y' / tg(2\theta) \qquad (7)$$

Where χ is the crab coefficient (of the order of one or less), x(y) is the particle horizontal (vertical) coordinate, y' is the vertical slope.

3 DAΦNE UPGRADE HARDWARE MODIFICATIONS

Relevant modifications to the machine have been realized in 2007, aimed at implementing the new collision scheme, together with other hardware modifications involving injection kickers, bellows and beam pipe sections. A layout of the upgraded DAΦNE is shown in Fig. 4, and the main hardware changes are briefly illustrated in the following.

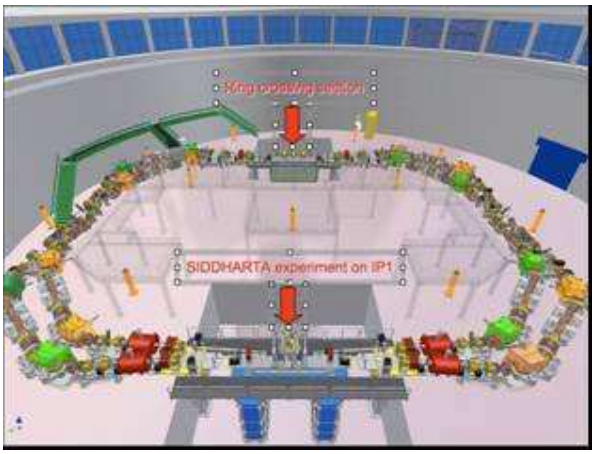

FIG. 4: Upgraded DAΦNE layout.

3.1 Interaction Regions layout

The KLOE Interaction Region (IR1) has been modified [6] for the installation of the Siddharta experiment, and equipped with new quadrupoles to be able to lower β^* at the IP. The total crossing angle has been increased from 30 mrad to 50 mrad, by removing the splitter magnets and rotating the two sector dipoles in the long and short arcs adjacent to the interaction regions of both rings. New beam pipes have been designed for this scheme. Existing sextupoles are used for the *CW* transformation. Fig. 5 shows the comparison between the KLOE IR1 layout (top) and the upgraded one (bottom).

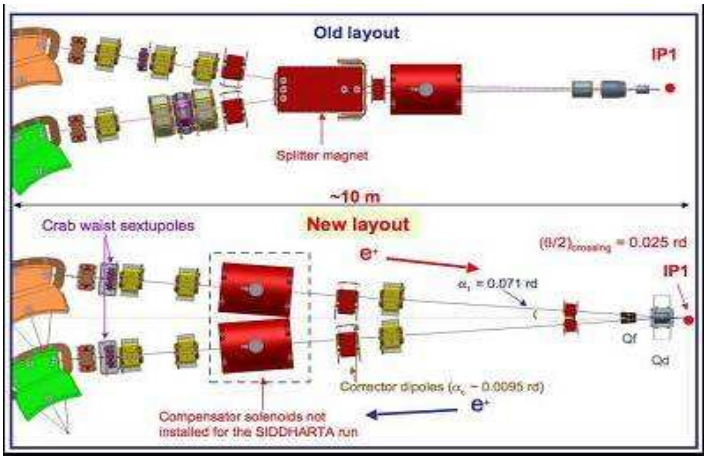

FIG. 5: Half view of old (top) and new (bottom) IR1 layout.

New permanent magnet quadrupole doublets are needed in order to focus the beams to the smaller β* at the IP. The first quadrupole of the doublet, QD0, is horizontally defocusing, and common to both beams in the same vacuum chamber: it provides a strong separation of the beams. The following horizontally focusing quadrupoles, QF1, are particularly small, in order to fit separated beam pipes for the two beams. The new configuration almost cancels the problems related to beam-beam long range interactions (PC), because the two beams experience only one parasitic crossing inside the defocusing quadrupole where, due to the large horizontal crossing angle, they are very well separated. Fig. 6 shows the pm quadrupoles in half IR and the beam pipe at the IP.

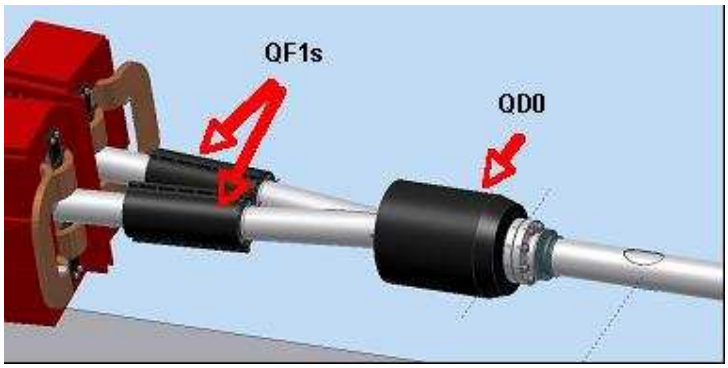

FIG. 6: Close up of the IP doublet.

The *CW* sextupoles are installed at both ends of the IR1. For the SIDDHARTA operation their intensity is more than a factor 5 larger than the average required for chromaticity correction in the ring. Four additional electromagnetic quadrupoles have been installed on both sides of IP1 to get the proper phase advance between the *CW* sextupoles and the IP. The compensator solenoids, present in the original KLOE setup, have been removed since there is no solenoid in the SIDDHARTA detector. However there is room to reintroduce them for a future KLOE run. In such a case, due to the new geometrical layout of IR1, two compensator solenoids will be necessary for each ring, requiring an upgrade of the cryogenic transfer lines.

The second IR (IR2) where the detector FINUDA was installed, has also been completely rebuilt, in order to provide full beam separation without low-β, and to be ready, with minor modifications, for a future FINUDA run based on the new collision scheme. A new beam pipe at IP2, providing complete separation between the two beams, has replaced the old one. This is geometrically symmetric to IR1, and its vacuum chamber is based on the same design criteria. Independent beam vacuum chambers are obtained by splitting the original pipe in two *half-moon* shaped sections, providing full vertical beam separation. The problem of the beam-beam long range interaction in this non colliding section is then naturally solved, allowing at the same time to relax the ring optics requirements imposed by beam separation at IP2. A view of half modified IR2 is in Fig. 7.

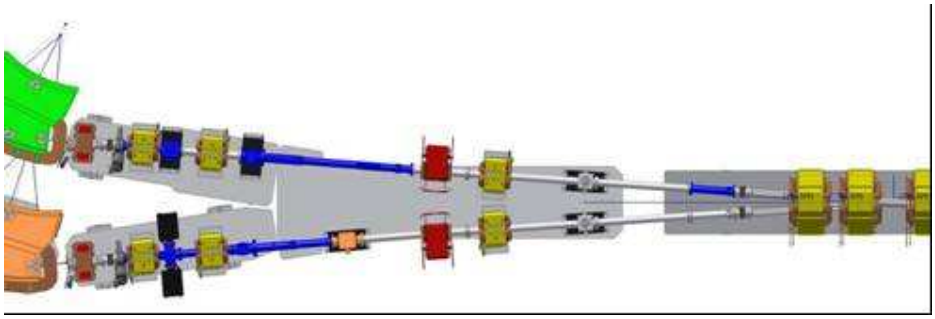

FIG. 7: View of the modified IR2 region (half).

In order to keep the ring coupling impedance low, all possible discontinuities have been avoided in the new vacuum chamber design. The number of bellows has been also limited to the strict necessary to compensate thermal strain and mechanical misalignments; there are four bellows per ring both in IR1 and in IR2.

3.2 Fast Injection kickers

New, fast kickers have been designed and built [7], based on a tapered strip with rectangular vacuum chamber cross section. The deflection is given by both the magnetic and the electric fields of a TEM wave traveling in the structure. Compared to the present DAΦNE injection kickers the new ones have a much shorter pulse (~12 ns instead of ~150 ns), better uniformity of the deflecting field, lower impedance and the possibility of higher injection rate (max 50 Hz). Moreover a smooth beam pipe and tapered transitions reduce the kicker contribution to the total ring coupling impedance. All these features should improve the maximum storable currents, colliding beams stability and backgrounds hitting the experimental detector during injection

3.3 New bellows

New bellows have been developed and installed in IR1 and in the ring. Four new bellows [8] are placed in each sector, connecting beam pipes with circular cross section. A RF shield is necessary to hide the chamber discontinuity to the beam. The coupling impedance of the structure has been evaluated in a frequency range from DC to 5 GHz and comes out to be very low. Simulations in this frequency range have shown that the new design reduces the bellows contribution to the ring coupling impedance.

3.4 Other modifications

Few ion clearing electrodes still installed on the electron ring and no longer necessary have been removed.

The transverse horizontal position of two wigglers in the long arcs has been moved by -2.5 mm in both rings, in order to reduce the non-linear terms in the magnetic field predicted by simulations and affecting the beam dynamics.

Positions of the electromagnetic quadrupoles, in the long straight sections on both

rings, have been changed to allow the installation of the new injection kickers and to provide a flexible configuration for tuning the phase advance between them.

The new ring layout is ~10 cm shorter than the original one, due to the removal of the splitter magnets and the requirement to keep the position of the arcs unchanged in order to minimize the implementation work. As a consequence, the frequency of the RF cavities has been changed by ~ 400 KHz. The variation is well within the tuner range of the rings RF cavities, but imposes some modifications on the Damping Ring (DR) operating conditions. In fact its RF cavity operates on a sub-multiple frequency of the Main Rings one, and the energy variation has to be corrected by changing the dipole field. The tuner range of the DR cavity has been then adapted in order to be compatible with the new operating conditions.

In Table I a comparison of the main beam parameters for the KLOE operation and the upgraded DAΦNE is presented.

TAB. 1: Comparison of beam parameters for KLOE and upgraded DAΦNE.

	DAΦNE KLOE	DAΦNE Upgrade
N_{bunch}	110	110
N_{part}/bunch	$2.65*10^{10}$	$2.65*10^{10}$
I_{bunch} (mA)	13.	13.
ε_x (nm)	400.	270.
ε_y (nm)	8	1.3
Coupling (%)	0.5	0.5
σ_x (μm)	775.	265.
σ_y (μm)	12.	3.4
σ_z (mm)	25.	20.
β_x (m)	1.5	0.26
β_y (mm)	18.	9.
θ (mrad)	2x16	2x26
Piwinski angle	0.36	2.5

4 FIRST RESULTS FROM THE UPGRADED DAΦNE COMMISSIONING

DAΦNE vacuum was closed in late November 2007. The operation restarted with a detuned optics, with ν_x slightly above 5, ν_y above 4 and *CW* sextupoles OFF, in order to speed up beam injection, to put the diagnostic in operation and to optimize the optics model. In December first beams were stored in the rings and installation of the luminosity monitors was completed. Redundancy in the luminosity measurement is required by the need to best quantify the luminosity gain obtained by adopting the new collision approach.

The new luminosity monitor for the collider consists of two different devices: a small angle Bhabha tile calorimeter split into 20 sectors (30 degrees each) made of alternating lead and scintillating tiles, covering a vertical acceptance between 17.5 and 27 degrees, and a GEM (Gas Electron Multiplier) tracker placed in front of the tile calorimeters allowing a redundant measurement of Bhabha events to minimize background. Fig. 8 shows a view of the luminosity monitors layout.

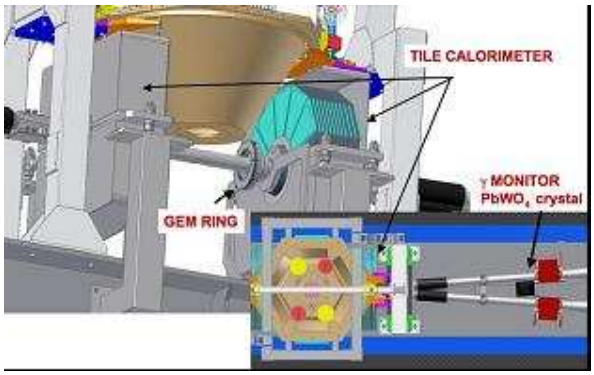

FIG. 8: View of the IP region with the luminosity monitors.

From January 2008 on there were continuous improvements on operation conditions with beams in collision, and once a reliable machine model had been defined the ring optics has been moved toward the nominal one having both tunes above 5. The transverse betatron coupling has been corrected mainly by rotating the permanent magnet focusing quadrupoles in IR1. The optimum obtained has been $\kappa \sim 0.5\%$ in both rings.

At the end of January the PM quadrupoles positions have been optimized and 2 electromagnetic quadrupoles have been added symmetrically with respect to the IP1 in order to meet the phase advance requirements imposed by the *CW* collision scheme. Present lattice has larger β^* values (β_x = 26 cm, β_y = 9 mm) with respect to design values.

At the beginning of February the first collision test with *CW* sextupoles started. Fig. 9 shows the electron (blue) and positron (red) beam sizes as measured by the Synchrotron Light Monitor (SLM). The bump in the electron horizontal and vertical beam sizes corresponds to the blow-up of the beam when the *CW* sextupoles in the electron ring where switched OFF (positron ring *CW* sextupoles were always ON). When switching them ON the beam conditions are restored.

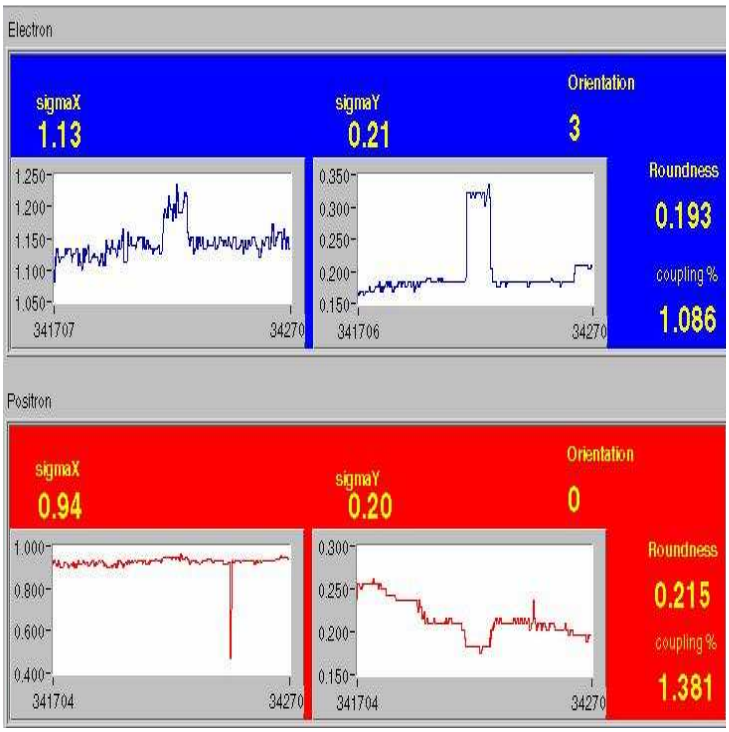

FIG. 9: Beam sizes (e^- blue, e^+ red) as measured by the Synchrotron Light Monitor (SLM). The bump corresponds to the *CW* sextupoles switched OFF

At the same time the Bhabha counter showed a dip in the counting rates, corresponding to a loss of luminosity due to the electron beam blow-up (Fig. 10). The corresponding lifetime increase is also due to the blow-up of the beam dimensions, being lifetimes dominated by the Tousheck effect.

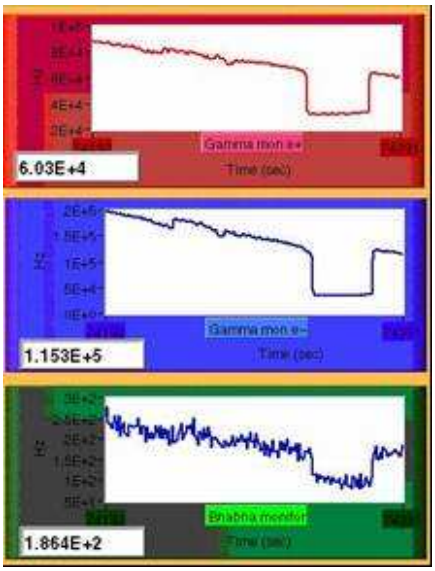

FIG. 10: Bhabha rates from the EMC. Dip corresponds to *CW* sext. switched OFF

In order to overcome the problem of a horizontal instability in the positron beam, limiting the maximum storable current and probably due to e-cloud, in February solenoid windings with ~ 45 Gauss field have been installed in both IRs and in some sections of the positron ring. About 800 mA of positrons were then stored in 60 bunches arranged in 12 bunch trains.

The SIDDHARTA detector was installed in March, providing a further luminosity monitor with the number of Kaon pairs detected. An energy scan has been performed in order to set the machine energy exactly at the Φ resonance peak.

The convolved IP vertical beam size in collision has been measured by means of a beam-beam scan technique. A measured Σ_y of 5.6 μ is compatible with the value obtained by using the coupling value (κ~0.7%) as measured at the SLM, being the single vertical beam size at the IP1 of the order of 4 μ.

Background rates have been optimized by adjusting the beam orbit, the collimators position, adding lead shielding especially in the IR1, and tuning the colliding beam positions. The total background seems to be strongly dominated by the beams parameter in the rings, and is considerably higher than during the last DAΦNE run.

The luminosity as a function of the product of currents presents a linear behaviour, as expected. Specific luminosity is higher than during the past best runs, as also expected (see Fig. 11 and 12). Maximum measured peak luminosity was of the order of $2x10^{32}$ $cm^{-2}s^{-1}$, with about 800 mA of electrons and 600 mA of positrons.

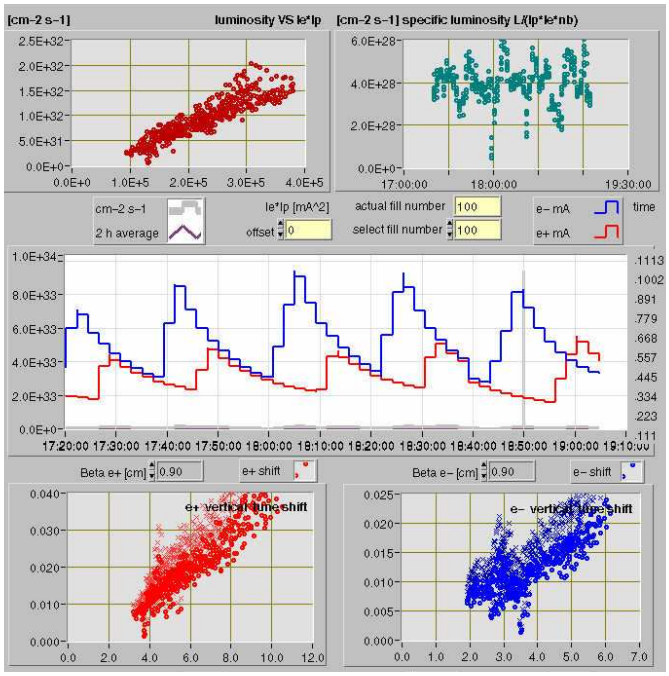

FIG. 11: Luminosity vs product of beam currents (top left), specific luminosity vs time (top right), beam currents vs time (medium plot, blue electrons, red positrons) and tune shifts vs bunch current (bottom plots) for a run. of SIDDHARTA experiment.

As a comparison, in Fig. 12 are the same plots for the first KLOE IR setup (2002, three quadrupoles in the low-β region) and the second one (2005, two quadrupoles in the low-β).

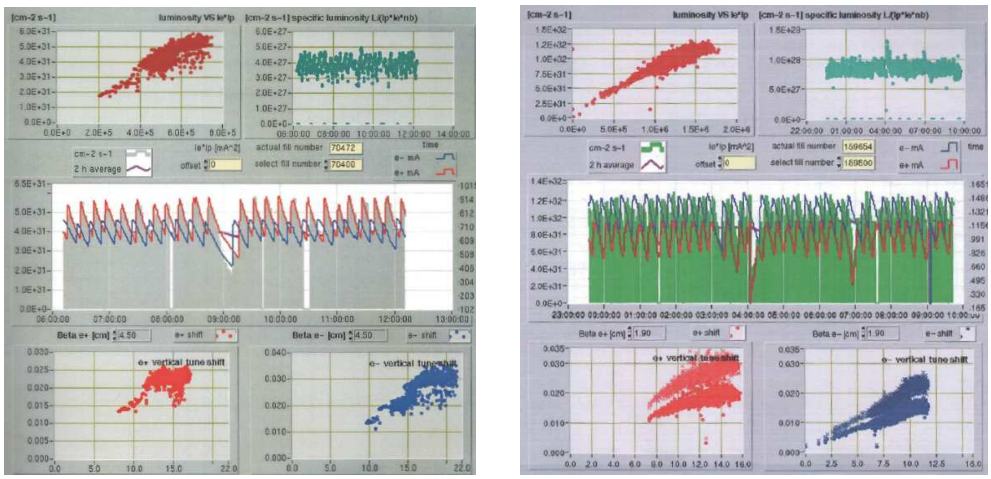

FIG. 12: Same plots as in Fig. 11 for KLOE in 2002 (left) and in 2005 (right).

The commissioning of the upgraded DAΦNE is still going on. Presently all efforts are aimed at improving the luminosity monitor reliability, the maximum beam currents, and lifetimes.

5 PROJECTION TO *SuperB*

The first DAΦNE results are very encouraging for present and future colliders.

The *SuperB* accelerator project, which is based on the same concept, will greatly profit from the experience gained at DAΦNE.

By increasing the number of bunches higher luminosity can be achieved, the main limitation being then due to wall power. With a RF power of 58 MW a luminosity up to $4x10^{36}$ cm^{-2} s^{-1} can be obtainable by doubling the number of bunches. Resulting injection rate is then doubled with respect to the upgrade parameters.

In Table II the main *SuperB* beam parameters are summarized for the Nominal and Upgrade configurations.

TAB. 2: *SuperB* main parameters (Nominal and Upgrade phase)

	Nominal		Upgrade	
PARAMETER	LER (e+)	HER (e-)	LER (e+)	HER (e-)
Energy (GeV)	4	7	4	7
Luminosity x 10^{36}	1.0		2.0	
Circumference (m)	1800	1800		
Revolution frequency (MHz)	0.167			
Eff. long. polarization (%)	0	80		
RF frequency (MHz)	476			
Momentum spread (x10^{-4})	7.9	5.6	9.0	8.0
Momentum compaction (x10^{-4})	3.2	3.8	3.2	3.8
Rf Voltage (MV)	5	8.3	8	11.8
Energy loss/turn (MeV)	1.16	1.94	1.78	2.81
Number of bunches	1251			
Particles per bunch (x10^{10})	5.52			
Beam current (A)	1.85			
Beta y* (mm)	0.22	0.39	0.16	0.27
Beta x* (mm)	35	20		
Emit y (pm-mrad)	7	4	3.5	2
Emit x (nm-mrad)	2.8	1.6	1.4	0.8
Sigma y* (microns)	0.039	0.039	0.0233	0.0233
Sigma x* (microns)	9.9	5.66	7	4
Bunch length (mm)	5		4.3	
Full Crossing angle (mrad)	48			
Wigglers (#) 20 meters each	0	0	2	2
Damping time (trans/long)(ms)	40/20	40/20	28/14	28/14
Luminosity lifetime (min)	6.7		3.35	
Touschek lifetime (min)	13	20	6.9	10.3
Effective beam lifetime (min)	4.5	5.1	2.3	2.5
Injection rate pps (x10^{11}) (100%)	2.6	2.3	5.1	4.6
Tune shift y (from formula)	0.15		0.20	
Tune shift x (from formula)	0.0043	0.0025	0.0059	0.0034
RF Power (MW)	17		25	

In Fig. 13 expected *SuperB* peak and integrated luminosities are presented as a function of the years of operation.

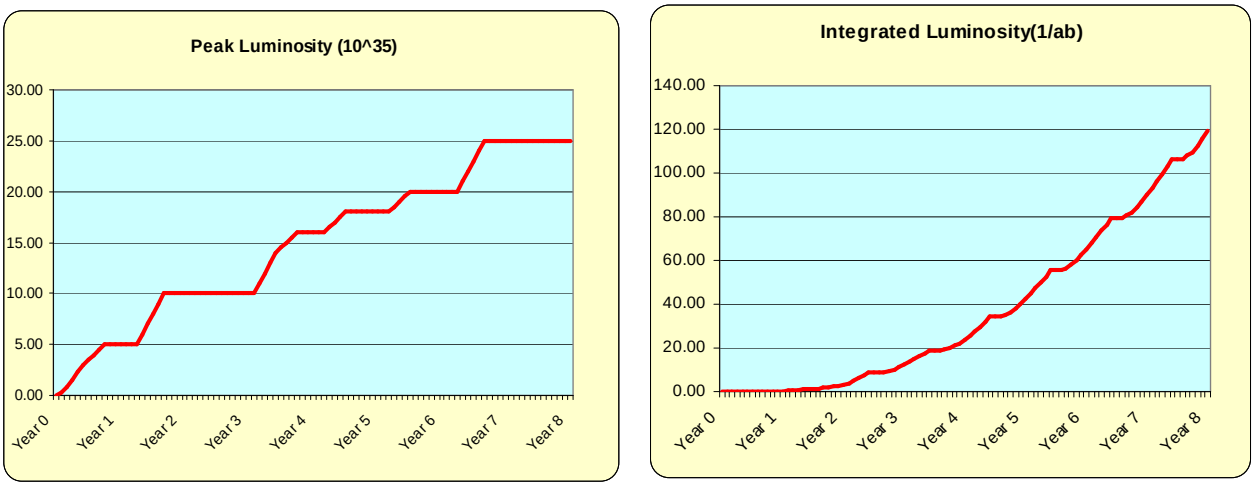

FIG. 12 The expected peak (left) and integrated (right) luminosities of *Superb* after the start-up in year 0.

8 REFERENCES

(1) Y. Ohnishi, "Upgrade plan of KEKB, from 2012 to 20XX", talk at BNM2008, 3rd International Workshop "B Factories and New Measurements", Atami (Japan), January 24-26 2008.

(2) P.Raimondi, D.Shatilov, M. Zobov, physics/0702033, (2006).

(3) P. Raimondi, M. Zobov, DAΦNE Techn. Note G-58, (2003); D. Shatilov, M. Zobov, ICFA Beam Dynamics Newsletter 37:99-109, (2005).

(4) D.V. Pestrikov, "Vertical Synchrobetatron Resonances due to Beam-Beam Interaction with Horizontal Crossing", Nucl. Instrum. Meth. A336:427-437, (1993).

(5) K. Ohmi et al., "Luminosity Limit due to the Beam-Beam Interactions with or without Crossing Angle", Phys. Rev. ST Accel. Beams **7**:104401, (2004).

(6) S. Tomassini et al, "DAΦNE upgrade: a new magnetic and mechanical layout", Proc. of 2007 Particle Accelerators Conference, Albuquerque (US), (2007).

(7) D. Alesini et al., "Fast Injection Kicker for DAΦNE and ILC Damping Rings", DAΦNE Techn. Note I-17, (2006).

(8) F. Marcellini, "Design and Electromagnetic analysis of the new DAΦNE interaction region", Proc. of 2007 Particle Accelerators Conference, Albuquerque (US), (2007)

(9) SuperB Conceptual Design Report, arXiv:0709.0451 [hep-ex] (2007).